


## RESEARCH ARTICLE

# PECCO: A profit and cost-oriented computation offloading scheme in edge-cloud environment with improved Moth-flame optimization

Jiashu Wu<sup>1,2</sup>  | Hao Dai<sup>1,2</sup> | Yang Wang<sup>1</sup>  | Shigen Shen<sup>3</sup>  | Chengzhong Xu<sup>4</sup>

<sup>1</sup>Shenzhen Institute of Advanced Technology, Chinese Academy of Sciences, Shenzhen, China

<sup>2</sup>University of Chinese Academy of Sciences, Beijing, China

<sup>3</sup>Shaoxing University, Shaoxing, China

<sup>4</sup>University of Macau, Macau, China

## Correspondence

Yang Wang, Shenzhen Institute of Advanced Technology, Chinese Academy of Sciences, 1068 Xueyuan Avenue, Shenzhen University Town, Shenzhen 518055, Guangdong, China. Email: [yang.wang1@siat.ac.cn](mailto:yang.wang1@siat.ac.cn)

## Funding information

Key-Area Research and Development Program of Guangdong Province, Grant/Award Number: 2020B010164002; Zhejiang Provincial Natural Science Foundation of China, Grant/Award Number: LZ22F020002

## Summary

With the fast growing quantity of data generated by smart devices and the exponential surge of processing demand in the Internet of Things (IoT) era, the resource-rich cloud centers have been utilized to tackle these challenges. To relieve the burden on cloud centers, edge-cloud computation offloading becomes a promising solution since shortening the proximity between the data source and the computation by offloading computation tasks from the cloud to edge devices can improve performance and quality of service. Several optimization models of edge-cloud computation offloading have been proposed that take computation costs and heterogeneous communication costs into account. However, several important factors are not jointly considered, such as heterogeneities of tasks, load balancing among nodes and the profit yielded by computation tasks, which lead to the profit and cost-oriented computation offloading optimization model *PECCO* proposed in this article. Considering that the model is hard in nature and the optimization objective is not differentiable, we propose an improved Moth-flame optimizer *PECCO-MFI* which addresses some deficiencies of the original Moth-flame optimizer and integrate it under the edge-cloud environment. Comprehensive experiments are conducted to verify the superior performance of the proposed method when optimizing the proposed task offloading model under the edge-cloud environment.

## KEYWORDS

cloud computing, edge-cloud computation offloading, Internet of Things, Moth-flame optimizer

## 1 | INTRODUCTION

With the rapid prevalence of smart devices<sup>1</sup> such as mobile phone and Internet-of-Things (IoT) devices,<sup>2-4</sup> a vast amount of data has been generated<sup>5,6</sup> and the demand of computation resources has been boosted.<sup>7,8</sup> Due to the limited computation, storage, and energy capacity of these smart devices,<sup>9</sup> the powerful *cloud computing* has been leveraged to provide elastic on-demand services to cope with limitations of smart devices.<sup>10,11</sup> With the support of resource-rich cloud servers, processing and storage-intensive applications such as augmented reality (AR)<sup>12</sup> and virtual reality (VR)<sup>13</sup> become feasible.

However, the fast growing of computation demands pose severe burden on cloud centers,<sup>14-16</sup> and tremendous amount of data generated<sup>5,17</sup> congests the network with limited bandwidth,<sup>15,16,18</sup> hence causing bottlenecks for the cloud-based computing paradigm. To relieve the pressure on cloud centers, the *edge computing* concept has emerged,<sup>15,19,20</sup> which allows computation to be performed at the edge network. The *Edge network*<sup>16</sup>

refers to the computing and network resources sit along the path between data sources and cloud centers. The rationale of *computation offloading*<sup>21,22</sup> is to let the computation happen at closer proximity to the data sources, so that not only the load pressure of cloud centers can be lessened, but also the quality of service can be improved as the edge computing can provide more efficient responses.<sup>23</sup>

To fully excavate the potential of edge-cloud computation offloading, several past research efforts investigated performance-influencing factors and proposed optimization models to maximize the performance gain while not causing significant costs. Wang et al.,<sup>24</sup> presented a two-phase optimization algorithm and an iterative improvement algorithm to jointly optimize the computation costs and latency under the mobile-edge setting. Li et al.,<sup>25</sup> constructed a cost graph to optimize the energy consumption of handheld computing devices during computation offloading to achieve considerable energy saving. Works in References 24,26–28 all considered optimizing the communication cost under the edge-cloud task offloading setting. Specifically, they adopted a homogeneous communication model with two assumptions: cloud-cloud and edge-edge communication cost were ignored, and the edge-cloud and cloud-edge communications were assumed to have symmetric costs, irrespective of the communication direction and distance between nodes. To address the over-simplicity of homogeneous communication models in these methods, Du et al.,<sup>21</sup> attempted the heterogeneous communication model and proposed HETO algorithm that can jointly minimize the computation, communication, and migration costs during computation offloading. Their work was the first to propose a heterogeneous communication model so that the deficiencies in existing researches can be overcome.

Despite various attempts of past researches to optimize the edge-cloud computation offloading problem, these models still suffered from the following drawbacks:

- These methods were not fine-grained enough. Although some methods considered heterogeneous communication cost, these methods failed to leverage more fine-grained factors such as the distance between node pairs. These methods also only leveraged a homogeneous cost model for computation tasks, which did not reflect the task heterogeneity in real-world settings.
- During computation offloading, some methods did not pay attention to the load balancing, which can cause overloading on certain nodes.
- These methods were cost-oriented, which failed to jointly optimize the profit and cost during computation offloading.

To address these issues, we propose a novel edge-cloud computation offloading model which not only utilizes the more realistic heterogeneous communication and computation cost model, but also considers the cost and profit heterogeneities of tasks. Hence, the proposed method jointly optimizes the profit and cost yielded during computation offloading. The model is named as *PECCO*, which stands for “Profit and Cost-oriented Edge-Cloud Computation Offloading.”

Considering this optimization problem is hard in nature and the objective of the *PECCO* model is not differentiable, we consider using the Moth-flame optimization (MFO) algorithm<sup>29</sup> to tackle the computation offloading problem. As a swarm-based algorithm, it is gradient-free and it balances exploration and exploitation. Besides, empirically it outperforms other swarm-based counterparts in terms of convergence speed<sup>29</sup> and so forth, which make it suitable to be leveraged in this case. We therefore propose an improved Moth-flame optimizer (*PECCO-MFI*) that addresses several drawbacks of the original MFO and significantly boosts its optimization effectiveness. Specifically, a density-aware Moth-flame initializer is designed to fit under the edge-cloud computation offloading setting. A dynamic hierarchical flaming mechanism is applied to avoid the single flame matching which is more likely to cause local optima stagnation. Moreover, the lifetime of moths is introduced to promote exploration when the corresponding paired flame is eliminated.

In summary, this article makes the following contributions:

- We construct a profit and cost-oriented edge-cloud computation offloading optimization model *PECCO* that jointly optimizes both the heterogeneous profit of computation tasks and the heterogeneous cost produced during computation offloading.
- We not only utilize the heterogeneous communication cost, but also consider the load balancing among nodes during optimization.
- We realize the suitability to leverage the Moth-flame optimizer, and propose an improved algorithm which tackles several deficiencies of the original MFO and hence boosts the effectiveness when solving the proposed computation offloading model.

The rest of the article is organized as follows, Section 2 introduces some related works on both edge-cloud computation offloading models and optimization algorithms. The research opportunities are then discussed. The background, suitability, and room for improvements to the MFO algorithm are given in Section 3. Section 4 presents the details of the proposed model, as well as how the MFO algorithm is improved and integrated. Section 5 presents the experimental settings and results to verify the effectiveness of the proposed algorithm when tackling the proposed model. Section 6 concludes the article.

## 2 | RELATED WORK

In this section, past research works on edge-cloud computation offloading models will be presented. Then, some well-known optimizers will be presented and compared. Finally, the research opportunities of our work are discussed.

## 2.1 | Offloading model

As a promising technique that can relieve the burden posed on cloud centers, edge-cloud computation offloading has drawn huge attention from both industry and academic community.<sup>9,30</sup> Wu et al.,<sup>27</sup> formulated the edge-cloud computation offloading problem into a graph min-cost partitioning problem, in which computation tasks will be partitioned to be run on either the cloud side or the edge side. The proposed min-cost offloading partitioning algorithm took both the execution time and energy consumption into account when deciding an optimal task partitioning strategy. Li et al.,<sup>25</sup> put forward a partition scheme to offload computation tasks on handheld devices. A cost graph was constructed and the partition scheme was applied to split computation programs into server tasks and client tasks with the aim to reduce the energy consumption. Juttner et al.,<sup>26</sup> presented the Lagrange relaxation based aggregated cost (LARAC) algorithm, which formulated a task graph and traversed the shortest path between nodes when considering the communication costs. The proposed algorithm was effective on delay-sensitive applications, justified by the simulation experiment they performed.

In works completed by Wang et al.,<sup>24</sup> and Dong et al.,<sup>28</sup> they paid attention to the communication cost faced in the edge-cloud computation offloading problem. When modeling the communication cost, communications between nodes on the same side (cloud-cloud, or edge-edge) were assumed to be cost-free. Moreover, to simplify the model, communication costs were assumed to be symmetric, that is, cloud-edge and edge-cloud communications have the same cost, irrespective of direction and the distance between nodes on different sides. The homogeneous communication model they leveraged is considered to be over-simplified and highly infeasible in real-world settings, as the cost can be asymmetric and distance-dependent. Therefore, Du et al.,<sup>21</sup> proposed a more fine-grained heterogeneous cost model, in which the symmetric assumption was relaxed, and the communication costs between nodes in a single side were no longer ignored. They then formulated the problem as a graph partitioning problem and designed the HETO algorithm to find a sub-optimal offloading strategy. Experiments on PageRank datasets testified to the excellent performance of the HETO algorithm when minimizing the communication, computation, and migration costs.

Despite that various research efforts have been drawn to optimize the edge-cloud computation offloading, they still suffered from some drawbacks which need to be addressed:

- Although the heterogeneous communication cost has been considered in some works, they failed to leverage more fine-grained factors such as distance between node pairs.
- When considering the cost during computation offloading, these methods utilized a homogeneous cost model for computation tasks, that is, task heterogeneity was ignored.
- During computation offloading, some methods did not take load balancing into consideration, that is, some node may be overloaded.
- These methods were cost-oriented, which failed to jointly optimize the profit and cost during computation offloading.

## 2.2 | Model optimizer

A suitable optimizer is indispensable to tackle the edge-cloud computation offloading problem and find out an excellent offloading strategy. Some well-known individual-based optimization algorithms were proposed.<sup>31,32</sup> They only optimized a single search candidate, and hence enjoyed a lighter computation cost and required less function evaluations. For instance, Lawrence<sup>33</sup> presented the Hill Climbing (HC) algorithm which iteratively improved a single search candidate by changing its variables. The Iterated Local Search (ILS) algorithm proposed by Lourenco et al.,<sup>34</sup> was an improvement towards the HC algorithm. The best solution obtained in each iteration was perturbed and utilized as the starting point of the next iteration. Despite the efficiency enjoyed by these algorithms, they suffered a lot from the local optima stagnation. These algorithms may encounter the premature convergence, which prevents them from converging towards the global optima. Some more advanced algorithms such as gradient descent<sup>35</sup> have also been widely applied, especially for the optimization in the field of deep learning.<sup>36,37</sup> However, these methods required gradient information of the objective function, which made them not applicable when the objective function is not differentiable.

In order to provide better local optima avoidance, some population-based optimization algorithms have been proposed and became popular in the past few years. By utilizing multiple search candidates and meanwhile balancing between exploration and exploitation, they provided higher possibilities to approach the global optima. As a sub-class of population-based algorithms, swarm-based algorithms<sup>38</sup> utilized multiple search candidates for the purpose of exploration. These search candidates then iteratively evolve, and eventually the healthier individuals will survive, making the exploitation become possible. Kennedy et al.,<sup>39</sup> presented the particle swarm optimization (PSO) algorithm that mimicked the behavior of birds in a flock which keep track of their individual and global best positions. The PSO involved only primitive math operations and was computationally inexpensive. Yang<sup>40</sup> proposed the firefly optimization algorithm (FFA), which was inspired by fireflies. During flying, fireflies are attracted by other fireflies with higher brightness. The effectiveness of the algorithm was verified on several test functions. A whale optimization algorithm (WOA) was proposed by Mirjalili et al.,<sup>41</sup> which was inspired by the bubble-net hunting strategy of humpback whales. The WOA algorithm mathematically

modeled this behavior to guide optimization. A grey wolf optimizer (GWO) was also proposed by Mirjalili et al.,<sup>42</sup> which modeled the social hierarchy of grey wolves during hunting to guide the optimization process. Besides, Mirjalili<sup>29</sup> put forward the MFO algorithm, which was one of the most famous swarm-based optimizers. The MFO utilized a population of moths to act as search candidates so that the probability of approximating the global optima was increased. Inspired by the transverse orientation characteristic of moths, the location of moths will be updated based on their transverse oriented path, with extra parameters controlling the exploration and exploitation. Each search candidate was iteratively assessed by a fitness function and hence the MFO algorithm was gradient-free. After several generation of evolvments, the fittest moth will be regarded as the optimized result. Experiments on several benchmarks<sup>29</sup> demonstrated that compared with several counterparts, the MFO algorithm can achieve better optimization results with statistical significance, while also converge in a fast manner.

### 2.3 | Research opportunity

Considering that past edge-cloud computation offloading models suffered from these aforementioned drawbacks, we find it promising to propose an optimization model that is both profit and cost-oriented. In terms of costs, the heterogeneous communication cost should be considered in a fine-grained manner. Moreover, a heterogeneous cost model should also be applied for tasks to make the model more practical. Besides, during computation offloading, load balancing should be taken care of to avoid computation node overloading.

A comprehensive optimization model and an excellent optimizer are both indispensable to produce a better task offloading strategy. Given the suitability of the MFO algorithm such as a higher chance to converge towards the global optima and its gradient-free merit, we propose an improved Moth-flame optimizer that addresses some design flaws of the original MFO, which can boost the effectiveness when working on the proposed computation offloading model.

## 3 | BACKGROUND

In this section, we first introduce the background of the MFO algorithm, including how it works, its advantages and its suitability to be utilized to solve the PECCO model. Then, some deficiencies of the MFO algorithm are pointed out which provide room for improvements for its improved version.

### 3.1 | The Moth-flame optimization algorithm

**Motivation and rationale** As a nature-inspired optimizer, the MFO algorithm is population-based as it involves a population of moths. The moth has a special navigation mechanism called *transverse orientation*, which they use as a flight path maintaining method. As shown in upper portion of the conceptual Figure 1, the moth attempts to maintain a fixed angle (marked in pink) between its flying direction and the moon, so that they can fly in a relatively straight path since the moon is far away from the moth. However, as illustrated in the lower part of Figure 1, the moth can sometimes

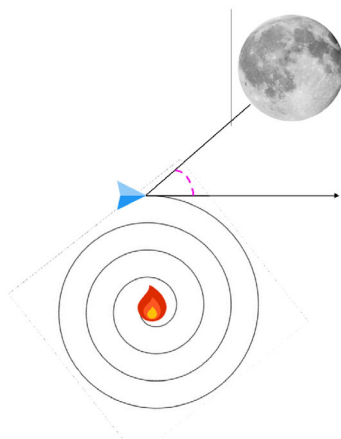


**FIGURE 1** Flight mechanism of the moth. The upper portion illustrates the *transverse orientation* mechanism. The lower portion illustrates the artificial light entrapment. The moth is represented using the blue arrow.

confuse the artificial light with the moon. Then, it will try to maintain the transverse orientation mechanism with the light which is much closer than the moon, leading to the entrapment towards the light and eventually hit it.

Inspired by this phenomenon, the MFO regards moths as search candidates, and treats the lights (flames) as potential optimal solutions. The MFO algorithm mimics the transverse orientation mechanism and hopes that the moth can reach the most optimal flame, which is regarded as the approximation to the global optima. By utilizing a population of moths instead of a single one, the Moth-flame optimizer possesses higher chance to avoid local optima entrapment and hence better approximates the global optima.

**General framework** The MFO algorithm works under the general framework of swarm-based algorithm.<sup>43</sup> The species population will first be initialized, then they will keep evolving, eliminating individuals with bad fitness and updating until the termination criteria are reached. Eventually, the fittest individual will survive and will be treated as the optimal solution.

**Formulation** The MFO algorithm involves  $n$  moths, each is a search candidate wandering in the search space. Each moth  $M_n \in \mathbb{R}^d$  is a  $d$  dimensional vector, where  $d$  is the number of features to be optimized. Hence, it leads to the moth matrix  $M$  with dimension  $n \times d$ , represented as follows:

$$M = \begin{bmatrix} M_1 \\ M_2 \\ \vdots \\ M_n \end{bmatrix} = \begin{bmatrix} m_{1,1} & m_{1,2} & \dots & m_{1,d} \\ m_{2,1} & m_{2,2} & \dots & m_{2,d} \\ \vdots & \vdots & \ddots & \vdots \\ m_{n,1} & m_{n,2} & \dots & m_{n,d} \end{bmatrix}. \quad (1)$$

A fitness function  $f$  is required to evaluate the fitness of each moth  $M_n$  by taking it as input, and returns its fitness, that is, the objective value. The objective function has the following formulation:

$$f : \mathbb{R}^d \rightarrow \mathbb{R}, f(M_n) = OM_n, \quad (2)$$

and hence, the corresponding fitness vector  $OM$  is defined as follows:

$$OM = \begin{bmatrix} f(M_1) \\ f(M_2) \\ \vdots \\ f(M_n) \end{bmatrix} = \begin{bmatrix} OM_1 \\ OM_2 \\ \vdots \\ OM_n \end{bmatrix}. \quad (3)$$

In the MFO algorithm, the flames are not the real flames in the real world. Instead, they are set to be moths with top  $k$  highest fitness values that have the right to survive (as in line 9 in Algorithm 3), hence the flame matrix  $F$  has dimension  $k \times d$ . Without prior knowledge about which moth location is better, initially, the MFO algorithm randomly initializes the flame matrix  $F$  with  $k = n$ . During iterations, the  $k$  will be gradually decreased as the population evolves. The flame matrix  $F$  is represented as follows:

$$F = \begin{bmatrix} F_1 \\ F_2 \\ \vdots \\ F_k \end{bmatrix} = \begin{bmatrix} f_{1,1} & f_{1,2} & \dots & f_{1,d} \\ f_{2,1} & f_{2,2} & \dots & f_{2,d} \\ \vdots & \vdots & \ddots & \vdots \\ f_{k,1} & f_{k,2} & \dots & f_{k,d} \end{bmatrix}, \quad (4)$$

and its corresponding fitness vector  $OF$  is defined as follows:

$$OF = \begin{bmatrix} f(F_1) \\ f(F_2) \\ \vdots \\ f(F_k) \end{bmatrix} = \begin{bmatrix} OF_1 \\ OF_2 \\ \vdots \\ OF_k \end{bmatrix}. \quad (5)$$

The details on how the MFO algorithm is integrated in the PECCO model, that is, what moth matrix  $M$  stands for and so forth, will be explained in Section 4.5.2.

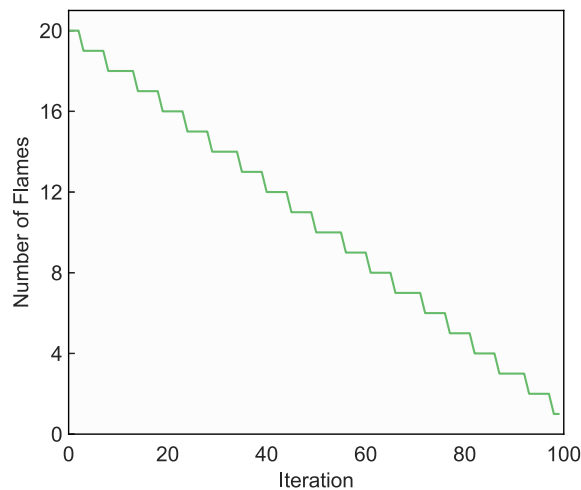


**FIGURE 2** Illustration of the decreasing trend of the number of flames  $k$ , that is, Equation (7).

As is previously mentioned, if there is no knowledge about which initial position is better, then a random initialization will be applied to generate both the moth matrix and the flame matrix using the following random generator:

$$m_{i,j} = (ub(i) - lb(i)) * random() + lb(i), \quad (6)$$

where  $ub$  and  $lb$  are the upper and lower bound of the range constraint, respectively. The  $random()$  function is a random number generator with range in  $[0, 1]$ .

**Deficiency 1:** The MFO algorithm applies a random initialization as it assumes there is no prior knowledge about which initial location is better. However, if prior knowledge presents, the random initialization will degrade the performance. Besides, the random initialization is not density-aware, that is, the random initialization may produce random vectors that are highly similar and hinder the diversity of the random population. An initial population with poor diversity will impair the benefit of population-based optimizers.

**Balancing exploration and exploitation** The MFO algorithm puts effort to balance between exploration and exploitation. Initially, there are  $n$  moths and  $n$  flames, each moth pursues its corresponding flame as illustrated by the solid arrows in Figure 3, which encourages exploration to avoid local optima stagnation as much as possible. During iterations, the moths will be sorted based on their fitness value in descending order, and the moths with top  $k$  highest fitness value will survive while other moths will be eliminated as shown in Algorithm 3. The value of  $k$  keeps decreasing based on the following formula during iterations so that the exploitation will be gradually emphasized:

$$k = round\left(n - Cl * \frac{n-1}{MI}\right), \quad (7)$$

where  $n$  is the initial number of moth/flame,  $MI$  denotes the total number of iterations (Max iteration),  $Cl$  stands for the current iteration. Eventually,  $k$  will decrease to 1, the last survived flame is regarded as the optimal solution produced by the MFO algorithm. The decreasing trend of  $k$  has been illustrated in Figure 2.

The number of flames  $k$  keeps decreasing while the number of moths  $n$  remains unchanged, the MFO algorithm therefore designs a moth-flame pairing mechanism as presented in Figure 3 so that the moths can decide which target flame is designated for them to pursue. At the beginning, the number of moths and flames are equal, that is,  $n$ , hence each moth will pursue its corresponding flame, that is,  $M_i \rightarrow F_i$ , as represented by the solid arrows in Figure 3. During iterations, the value of  $k$  will keep decreasing, hence the number of flames will be less than the number of moths. Under the MFO moth-pairing mechanism, the moth  $M_i$  will still pursue its corresponding flame  $F_i$  if flame  $F_i$  still survives, or otherwise  $M_i$  will chase the last flame  $F_k$  as represented by the dashed arrows in Figure 3.

**Deficiency 2:** During moth evolution, at any given time, moth  $M_i$  will always pursue a single designated flame, which increases the chance of being trapped in the local optima.

**Deficiency 3:** During moth evolution, those moths that have their corresponding flame being eliminated will always pursue the last surviving flame, which is the flame with the worst fitness. Neither pursuing the worst flame nor letting lots of moths pursuing a single flame is a reasonable design.

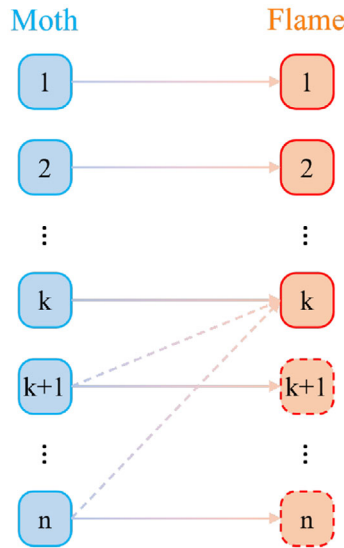


**FIGURE 3** The original moth-flame pairing mechanism. The moths are represented using blue boxes while the flames are represented using orange boxes.

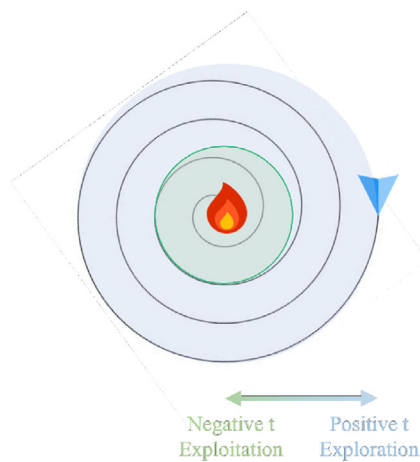


**FIGURE 4** Illustration of the exploration versus exploitation of the Moth-flame optimization algorithm

In terms of the moth updating mechanism, the MFO algorithm mimics the transverse orientation based on the following equation:

$$U(M_i, F_j) = D_{ij} \times e^{bt} \times \cos(2\pi t) + F_j, \quad (8)$$

where  $F_j$  is the paired flame designated for  $M_i$  to pursue,  $t$  is a random number in range  $[r, 1]$ ,  $r$  is a random number that will linearly decrease from  $-1$  to  $-2$  during iterations,  $b$  is the shape parameter, and  $D_{ij}$  denotes the  $L1$ -distance between  $M_i$  and  $F_j$  which is defined as follows:

$$D_{ij} = |F_j - M_i|. \quad (9)$$

The shape of an example updating path, that is, the spiral shape, has been illustrated in Figures 1 and 4.

Specifically, the  $t$  parameter decides how close to the flame will the moth's terminal position be. As illustrated in Figure 4, a  $t$  value that is closer to 1 will let the moth ends up with a position that is farther from the flame (the blue shaded area), which emphasizes exploration. On the other hand, a negative  $t$  value will draw the moth closer towards its target flame as indicated by the green shaded area in Figure 4, which encourages exploitation. Since  $t$  is within the range of  $[r, 1]$ , initially,  $r$  has value  $-1$  which promotes exploration by avoiding the moth to be too close to the flame. As the process evolves,  $r$  linearly decreases from  $-1$  to  $-2$ , which gradually encourages exploitation over exploration.

**Termination** The termination criterion is when there is only one flame remaining. It will be treated as the optimal solution.

**Advantage and applicability** In summary, the MFO algorithm has the following advantages which make it applicable in our case:

- Since the *PECCO* model is hard in nature, applying this population-based algorithm with multiple search candidates while enabling the balance between exploration and exploitation will possess higher chance to approximate the global optima.
- Since the objective function in the *PECCO* model is not differentiable, the Moth-flame optimizer becomes applicable as it evaluates each search candidate using the fitness function and therefore is gradient-free.
- Compared with its counterparts, the Moth-flame optimizer achieves superior optimization results and converges in an efficient manner.

**Room for improvements** As is aforementioned, the MFO algorithm suffers from three deficiencies, which leave us with room for improvements. We propose three new mechanisms to tackle these deficiencies as follows:

- The profit, cost, and density-aware initializer → Deficiency 1
- The dynamic hierarchical flaming mechanism → Deficiency 2
- The lifetime-enabled moth-flame pairing strategy → Deficiency 3

Together, these mechanisms form the improved *PECCO-MFI* algorithm. The details will be presented in Section 4.5.1.

## 4 | MODEL AND METHOD

In this section, the problem formulation will be provided, followed by the presentation of the proposed *PECCO* optimization model, in which the profit and cost component of the *PECCO* model will be explained. Then, we will explain how the MFO algorithm is improved and integrated to form our *PECCO-MFI* algorithm.

### 4.1 | Problem formulation

In the edge-cloud environment, there are cloud nodes and edge devices (nodes), with a connection topology to form a connected graph. Hence, we formulate the problem as a graph  $G = (V, E)$  where  $V$  stands for a set of cloud/edge nodes and  $E$  represents a set of communication links. There are in total  $N$  computing nodes, in which it contains  $I$  cloud nodes and  $J$  edge nodes, hence we have

$$\begin{aligned} V^C &= \{V_1^C, V_2^C, \dots, V_I^C\}, \quad V^E = \{V_{I+1}^E, V_{I+2}^E, \dots, V_{I+J}^E\} \\ V &= V^C \cup V^E, \quad V^C \cap V^E = \emptyset, \quad N = I + J. \end{aligned} \quad (10)$$

Note that we can simplify the notation  $V_n^X$ ,  $X \in \{C, E\}$  to be  $V_n$  as the range of subscript  $n$  can tell whether the node belongs to the cloud or the edge.

For each computing node  $V_n$ , it has the following properties. First, each computing node is capable of handling certain capacity of computation tasks. Hence  $Cap_{V_n-max}$  denotes the maximum number of units of computation workload that node  $V_n$  is capable of handling, while  $Cap_{V_n-min}$  stands for the minimum workload of node  $V_n$  when it is idle. We assume that no node can be overloaded by computation tasks. By considering the capacity of each node, it can also indirectly model other performance factors such as power consumptions.

As for edges  $E$  in the graph  $G$ , there are in total  $Q$  edges, denoted as  $E_q$ , or interchangeably  $E_{(V_s, V_t)}$ , which stands for edge  $E_q$  is an edge that starts from node  $V_s$  and points to node  $V_t$ . To make the heterogeneous model more generalizable, the length of each edge is also considered instead of being ignored as in References 21 and 26, and is denoted as  $L_{E_q}$  (or  $L_{E_{(V_s, V_t)}}$  using the interchangeable notation).

In terms of tasks to be executed, there are in total  $K$  of them, each task  $T_k$  has a property  $WL_{T_k}$  that represents how many units of computation workload does task  $T_k$  have. Each task can only be allocated on either a cloud node or an edge node, and a task is allowed to stay if its initial allocation is good enough. Hence, we define  $\mathcal{A}_{T_k}^I$  and  $\mathcal{A}_{T_k}^O$  to be the initial and offloaded allocation of task  $T_k$ , which satisfies

$$\mathcal{A}_{T_k}^I, \mathcal{A}_{T_k}^O \in V^X, \quad X \in \{C, E\}. \quad (11)$$



Moreover, vector  $\mathcal{A}^O$  is defined to represent the offloaded allocations of all  $K$  tasks as follows:

$$\mathcal{A}^O = \begin{bmatrix} \mathcal{A}_{T_1}^O \\ \mathcal{A}_{T_2}^O \\ \vdots \\ \mathcal{A}_{T_K}^O \end{bmatrix}. \quad (12)$$

Besides, the PECCO model applies a heterogeneous cost model for tasks. Instead of applying a homogeneous task cost as in Reference 21, for each task, it has different costs  $C_{T_k}^C$  if it is executed on the cloud, or  $C_{T_k}^E$  if being allocated to the edge. By utilizing a heterogeneous cost model for each task, it can reflect that different tasks can have different costs when being allocated to different sides, which makes the model more realistic. To make the model profit-oriented, each task is also associated with two profits, that is,  $P_{T_k}^C$  and  $P_{T_k}^E$ , which stand for the profit gained of completing task  $T_k$  on the cloud and edge, respectively. By jointly considering profit and cost, it makes the proposed PECCO model become profit and cost-oriented.

## 4.2 | PECCO cost model

The PECCO model is a multi-factored model that jointly considers both the generalized heterogeneous communication cost and the heterogeneous computation cost.

### 4.2.1 | Generalized heterogeneous communication cost model

Considering that previously proposed communication cost models in past researches suffered from several drawbacks (e.g., applied the unrealistic symmetric and cost-free assumption, failed to consider communication distance, applied homogeneous communication costs between node pairs and so forth) which made them become hardly generalizable in practice, it naturally leads to the rationale of our generalized heterogeneous communication cost model.

There are in general four types of communication costs, that is,  $w^{CC}$ ,  $w^{EE}$ ,  $w^{CE}$ , and  $w^{EC}$ . The CE here for instance represents the communication from a cloud node to an edge node. Inside each type of communication cost, it can also have different costs between different nodes, which is denoted as  $w_{(V_s, V_t)}^{XX}$ . For example,  $w_{(V_j^E, V_i^C)}^{EC}$  denotes the communication cost from edge node  $V_j^E$  to the cloud node  $V_i^C$ . As different nodes may work under different conditions like being operated by different service providers, the communication cost between node pairs can be different even if they are situated on the same side. Therefore, the model is more realistic in practice. This kind of generalization also offers convenience to represent communication failures for instance, by setting the edge-wise communication cost to be a large value. The communication cost function  $C_{E_{(V_s, V_t)}}$  is formulated as follows:

$$C_{E_{(V_s, V_t)}} = \text{sum} \left( L_{E_{(V_s, V_t)}} \times \left[ \mathbf{1}_{V_s, V_t \in V^C}, \mathbf{1}_{V_s, V_t \in V^E}, \mathbf{1}_{V_s \in V^C, V_t \in V^E}, \mathbf{1}_{V_s \in V^E, V_t \in V^C} \right] \odot \left[ w_{(V_s, V_t)}^{CC}, w_{(V_s, V_t)}^{EE}, w_{(V_s, V_t)}^{CE}, w_{(V_s, V_t)}^{EC} \right] \right), \quad (13)$$

inside it, for instance,  $\mathbf{1}_{V_s \in V^C, V_t \in V^E}$  will return 1 if  $V_s$  is a cloud node and  $V_t$  is an edge node, and will return 0 otherwise, other indicator functions carry the similar meaning. The  $\odot$  represents the element-wise multiplication operator and  $\times$  is the scalar multiplication operator. Hence, the communication cost function  $C_{E_{(V_s, V_t)}}$  will return the length of the inputted edge times the corresponding cost of that type of communication so that the heterogeneous communication costs between node pairs can be considered.

After defining the generalized heterogeneous communication cost model, the optimal cost path between any pairs of computing nodes can be pre-computed using the shortest path algorithm. The optimal cost path between node  $V_i$  and  $V_j$  is denoted as  $OCP_{(V_i, V_j)}$ , and therefore we can define the optimal communication cost from node  $V_i$  to node  $V_j$  as follows:

$$\text{COMM}_{(V_i, V_j)} = \sum_{E_{(V_s, V_t)} \in OCP_{(V_i, V_j)}} C_{E_{(V_s, V_t)}}, \quad (14)$$

and therefore, the total communication cost is defined as follows:

$$\text{COMM}(G, T, \mathcal{A}^I, \mathcal{A}^O) = \text{argmin}_{\mathcal{A}^O} \left\{ \sum_{k=1}^K \text{COMM}_{(\mathcal{A}_{T_k}^I, \mathcal{A}_{T_k}^O)} \right\}. \quad (15)$$

The optimization algorithm should find an optimal offloading strategy  $\mathcal{A}^O$  to offload task  $T_k$  so that it can achieve a communication cost  $COMM(G, T, \mathcal{A}^O)$  as low as possible. In summary, the proposed generalized heterogeneous communication cost model overcomes the drawbacks of previously proposed communication models and has the following benefits:

- It no longer ignores the communication cost between nodes on the same side (i.e., cloud-cloud, edge-edge).
- The asymmetry between communication costs is considered, cost from cloud to edge and from edge to cloud communication can be heterogeneous.
- It considers distances when modeling communication cost between two nodes.
- It allows different node pairs to have heterogeneous communication costs.

## 4.2.2 | Heterogeneous computation cost model

Next, the heterogeneous computation cost model is defined which also takes the heterogeneities between computing tasks into account. Generally, for each task  $T_k$ , it possesses cost  $C_{T_k}^C$  and  $C_{T_k}^E$ , which is the cost of executing task  $T_k$  on the cloud and edge, respectively. Due to the diversity of tasks,  $C_{T_k}^C$  is not necessarily lower than  $C_{T_k}^E$ . The previously proposed homogeneous computation cost model for tasks is infeasible, it is unreasonable to assume that all tasks share exactly the same computation cost when being executed on a single side. Hence, the computation cost model for tasks we considered in the PECCO is more generalizable. The overall computation cost is formulated as follows:

$$COMP(G, T, \mathcal{A}^O) = \operatorname{argmin}_{\mathcal{A}^O} \left\{ \sum_{k=1}^K \left( \mathbf{1}_{\mathcal{A}_{T_k}^O \in VC} \times C_{T_k}^C + \mathbf{1}_{\mathcal{A}_{T_k}^O \in VE} \times C_{T_k}^E \right) \right\}, \quad (16)$$

where the indicator function  $\mathbf{1}_{\mathcal{A}_{T_k}^O \in VC}$  will return 1 if the allocation for task  $T_k$   $\mathcal{A}_{T_k}^O$  is a cloud node, and will return 0 otherwise, similar for  $\mathbf{1}_{\mathcal{A}_{T_k}^O \in VE}$ .

## 4.3 | PECCO profit model

Different from previously proposed works, the proposed PECCO model is not only cost-oriented, but also profit-oriented. For each task  $T_k$ , it has profit  $P_{T_k}^C$  and  $P_{T_k}^E$  when being executed on the cloud and edge, respectively. The overall profit is formulated as follows:

$$PROFIT(G, T, \mathcal{A}^O) = \operatorname{argmin}_{\mathcal{A}^O} \left\{ \sum_{k=1}^K \left( \mathbf{1}_{\mathcal{A}_{T_k}^O \in VC} \times P_{T_k}^C + \mathbf{1}_{\mathcal{A}_{T_k}^O \in VE} \times P_{T_k}^E \right) \right\}. \quad (17)$$

## 4.4 | Overall optimization objective

Finally, the PECCO optimization model will integrate the aforementioned cost and profit model to become profit and cost-oriented. The objective function is defined as follows:

$$Obj(G, T, \mathcal{A}^O) = \operatorname{argmin}_{\mathcal{A}^O} \left\{ (COMM(G, T, \mathcal{A}^O) + COMP(G, T, \mathcal{A}^O)) + \lambda \times PROFIT(G, T, \mathcal{A}^O) \right\}, \quad (18)$$

where  $\lambda$  is a ratio parameter being set to a negative value to integrate the profit into the objective to be minimized. By having  $\lambda$ , the objective function can minimize the cost and simultaneously maximize the profit.

By jointly optimizing the profit and cost-oriented optimization model PECCO, we can find a solution that can jointly optimize costs and the profit as much as possible.

## 4.5 | The PECCO-MFI optimizer

In this section, we will introduce the proposed improved Moth-flame optimizer with detailed explanations to the improvements we made. Then, how the improved MFO algorithm is integrated to optimize the PECCO model is explained, that is, what moths stand for in the PECCO-MFI algorithm, how are tasks offloaded based on the optimized allocation strategy  $\mathcal{A}^O$  and so forth.

---

**Algorithm 1.** The profit, cost, and density-aware moth initializer  $initializer(nsa, G, T, ub, obj, \mathcal{A}^l)$  of the PECCO-MFI algorithm

---

**Input:**

Number of search candidates (moths)  $nsa$ ,  
 Edge-cloud graph  $G$ ,  
 Tasks  $T_k \in T$ ,  
 Allocation upper bound  $ub$ ,  
 Objective function  $Obj()$  as defined in Equation (18),  
 Initial allocation  $\mathcal{A}^l$

**Output:** Profit, cost, and density-aware moth initialization with dimension  $nsa \times N$

```

1: for  $T_k$  in  $T$  do
2:   Calculate costs based on Equations (15) and (16)
3:   Calculate the profit based on Equation (17)
4:   Calculate the profit and cost-oriented objective based on Equation (18)
5: end for
6: for  $i$  in  $range(nsa \times 1.5)$  do
7:   for  $k$  in  $range(K)$  do
8:     if allocate task  $T_k$  to the cloud side yield a lower objective value then
9:       Store random number in range  $[0, \frac{ub}{2})$  into  $\mathcal{A}_i^l$ 
10:    else
11:      Store random number in range  $[\frac{ub}{2}, ub]$  into  $\mathcal{A}_i^l$ 
12:    end if
13:  end for
14: end for
15: while  $len(\mathcal{A}^l) \neq nsa$  do
16:   Find pair  $(\mathcal{A}_i^l, \mathcal{A}_j^l)$  with minimum intra-pair L2 distance
17:   Add  $\frac{\mathcal{A}_i^l + \mathcal{A}_j^l}{2}$  into  $\mathcal{A}^l$ 
18:   Remove both  $\mathcal{A}_i^l$  and  $\mathcal{A}_j^l$  from  $\mathcal{A}^l$ 
19: end while
20: return  $\mathcal{A}^l$ 

```

---

#### 4.5.1 | Algorithm improvement

To tackle the deficiencies mentioned in Section 3.1 and therefore boost the performance, we propose an improved Moth-flame optimizer called PECCO-MFI with three improvements to tackle three deficiencies, respectively.

**Improvement 1 (Profit, cost, and density-aware Moth initializer):** To tackle the *Deficiency 1: trivial random initialization*, we design a new moth initializer that is profit, cost, and density-aware, as shown in Algorithm 1.

*Profit and cost-awareness:* The newly designed moth initializer will allocate tasks (elements in each moth) to cloud or edge side based on their profit and cost. It is natural to allocate services to the side in which they possess a lower profit-cost objective than the other side. Conversely, if the allocation is done in the reversed way, then this task is likely to be migrated during the optimization process, which therefore incurs unnecessary costs. The profit and cost-aware moth initialization mechanism has been shown in lines 7–13 in Algorithm 1. By utilizing this prior knowledge, the improved MFO algorithm is reasonable to outperform its knowledgeless random counterpart.

*Density-awareness:* The rationale of applying the population-based paradigm is to maximize the chance of approximating the global optima as close as possible. However, if some moths are initialized to have a close proximity, the benefit of the population-based paradigm will be greatly hindered. To ensure the initialized moths have rich diversity, the newly designed initializer will generate more moth vectors than required, then it will iteratively remove the closest pair of moths and keep the average of them. The procedure has been given in lines 15–19 in Algorithm 1. The removal will be continued until the number of moth vectors is satisfied as required. By leveraging this mechanism, moth vectors that are initialized to be too close will be merged into a new one to prevent the performance degradation from happening. Therefore, the proposed moth initializer is density-aware.

**Improvement 2 (Dynamic hierarchical flaming mechanism):** To deal with the *Deficiency 2: Single moth-flame pairing*, a dynamic hierarchical flaming mechanism is applied. As pursuing a single flame will lead to higher risk of being trapped in local optima, inspired by the social hierarchy

**Algorithm 2.** The dynamic hierarchical flaming mechanism and the lifetime-enabled moth-flame pairer *enhanced\_pairer(CI, MI)* of the PECCO-MFI algorithm

**Input:**

Current iteration  $CI$ ,

Max iteration  $MI$

- 1: Define  $F_1, F_2, F_3$  as the flames with top 3 fitness values, respectively
- 2:  $\omega \leftarrow \frac{CI}{MI}$
- 3: **if** moth  $M_i$ 's corresponding flame  $F_i$  still survives **then**
- 4:   **if** there are  $\geq 3$  flames survive **then**
- 5:      $M_i$  will pursue  $\frac{F_i + \omega \times F_1 + \omega \times F_2 + \omega \times F_3}{1 + 3 \times \omega}$
- 6:   **else if** there are 2 flames survive **then**
- 7:      $M_i$  will pursue  $\frac{F_i + \omega \times F_1 + \omega \times F_2}{1 + 2 \times \omega}$
- 8:   **end if**
- 9: **else**
- 10:    $\tau \leftarrow \text{random}(0, 1)$ , where  $\tau$  is the lifetime parameter
- 11:   **if**  $\tau > 0.8$  **then**
- 12:      $F_I \leftarrow$  a randomly initialized flame
- 13:   **else**
- 14:      $I \leftarrow \text{random}(0, k)$
- 15:   **end if**
- 16:   **if** there are  $\geq 3$  flames survive **then**
- 17:      $M_i$  will pursue  $\frac{F_I + \omega \times F_1 + \omega \times F_2 + \omega \times F_3}{1 + 3 \times \omega}$
- 18:   **else if** there are 2 flames survive **then**
- 19:      $M_i$  will pursue  $\frac{F_I + \omega \times F_1 + \omega \times F_2}{1 + 2 \times \omega}$
- 20:   **end if**
- 21: **end if**

possessed in the moth species, the moths with top 3 highest fitness values will be regarded as leaders, which will provide guiding reference for other moths to pursue. Hence, instead of pursuing a single flame, in the newly designed algorithm, each moth will chase the linear combination of its designated flame and the leader flames, as shown in lines 3–8 in Algorithm 2.

**Exploration and exploitation balance:** At the beginning of the training process, putting too much dependency on the top 3 flames will incur risk of local optima stagnation as the performance of flames at the beginning is not promising enough. Hence, an adjusting factor  $\omega$  is introduced which linearly increases from 0 to 1 during the training process as indicated in line 2 in Algorithm 2. After applying the adjusting factor  $\omega$  as in lines 5 and 7 in Algorithm 2, exploration will be encouraged at the beginning by putting less emphasis on the top 3 flames since initially the value of  $\omega$  is small. As the training progresses,  $\omega$  will gradually increase, which will emphasize more exploitation, since the guiding reference of top 3 flames will be gradually reinforced as the  $\omega$  keeps growing. As such, the utilization of adjusting factor  $\omega$  in the newly designed dynamic hierarchical flaming mechanism will balance between exploration and exploitation.

**Improvement 3 (Lifetime-enabled Moth-flame pairing strategy):** Finally, to solve the *Deficiency 3: naive moth-flame pairing*, we design a fairer pairing strategy as indicated in lines 9–21 in Algorithm 2. Instead of letting all moths whose corresponding flames are eliminated to chase the last surviving flame, we introduce a lifetime parameter  $\tau$  with lifetime threshold set as 0.8. Due to the elimination of their unpromising flames, these moths are not promising themselves and hence the lifetime parameter  $\tau$  is used to decide whether certain moth will be re-initialized, that is, starting a new lifetime. Hence, as indicated in lines 11–12 in Algorithm 2, if the randomly generated lifetime parameter  $\tau$  is higher than the lifetime threshold, the moth will start a new lifetime by pairing with a newly initialized flame. Otherwise, the moth will continue its lifetime, and the algorithm will let it to pair with a randomly selected survived flame to promote a fairer exploration. By randomly pairing with a survived flame, these moths will fairly explore all possible survived flames instead of all exploiting the worst-fitted flame. During the re-pairing process, the aforementioned dynamic hierarchical flaming mechanism will be utilized again to provide better exploration and exploitation balancing while enabling the guiding reference of top 3 flames as in lines 16–20 in Algorithm 2. By utilizing this enhanced moth-flame pairing strategy, the exploration of the algorithm will be further encouraged and hence leading to a higher chance to approach the global optima.

**Algorithm 3.** Workflow of the *PECCO-MFI* algorithm**Input:**

Shape parameter  $b$ ,  
 Number of search candidates (moths)  $nsa$ ,  
 Allocation upper bound  $ub$ ,  
 Objective function  $Obj()$  as defined in Equation (18)

**Output:** Resource allocation strategy  $\mathcal{A}^o$  of computation tasks, which is the best flame  $F$

```

1: Initialize moth matrix  $M \leftarrow \text{initializer}(nsa, G, T, ub, obj, \mathcal{A}^l)$  (in Algorithm 1)
2:  $OM \leftarrow Obj(M)$ 
3: while  $len(F) \neq 1$  do
4:   Update  $k$ 
5:    $OM \leftarrow obj(M)$ 
6:   if  $CI = 1$  then
7:      $F \leftarrow M.sortBy(OM)$ 
8:   else
9:      $F \leftarrow M.sortBy(OM)[0 : k]$ 
10:  end if
11:  Update moth-flame pairing using enhanced_pairer( $CI, M$ ) (Algorithm 2)
12:  for  $i$  in  $range(nsa)$  do
13:    for  $j$  in  $range(K)$  do
14:      Update  $r$  and  $t$ 
15:      Calculate  $D$  with respect to the paired moth and flame using Equation (9)
16:      Update moth position using Equation (8)
17:    end for
18:  end for
19: end while
20:  $OF \leftarrow obj(F)$ 
21: return  $F, OF$ 

```

#### 4.5.2 | Integration of the Moth-flame optimizer

We apply the improved Moth-flame optimizer *PECCO-MFI* to optimize the *PECCO* model. The pseudocode of the algorithm has been presented in Algorithm 3. In the *PECCO-MFI* algorithm, each moth vector  $M_i$  is a  $1 \times K$  vector, where  $K$  is the number of tasks waiting to be allocated. The values in the moth vector  $M_i$  are within the range of  $[0, ub]$ , where  $ub$  is a constant. If the value is in range  $[0, \frac{ub}{2})$ , it indicates that this task will be executed to the cloud side, otherwise, this task will be offloaded to the edge side. Then, the algorithm will find the computing node with the cheapest communication cost in the designated side and allocate the task to that computing node. If the computing node will be overloaded by taking this task, the algorithm will find the node at the designated side with the second cheapest communication cost and so on. Eventually, the task will either be allocated to a computing node without causing overloading, or it will not be satisfied due to workload unavailability.

## 5 | EXPERIMENT

In this section, we will introduce our experimental setup and the dataset we utilized during experiments. Then, experimental results will be presented and explained to testify to the superiority of the proposed method. Specifically, objective values yielded by different methods are compared, followed by the comparison of profit, cost and profit-cost ratio to demonstrate the effectiveness of the *PECCO-MFI* algorithm in terms of joint profit and cost optimization. Finally, to demonstrate the *PECCO-MFI* algorithm offloads computation tasks wisely, the task allocation and the resource utilization are compared and analyzed.

### 5.1 | Dataset, parameter, and experimental setup

**Dataset.** The dataset we use to simulate the edge-cloud environment<sup>44</sup> is the Sydney train station parking dataset obtained from the Open Data Portal provided by the New South Wales Government Department of Transportation.<sup>45</sup> The dataset contains the parking lot availability information

at each train station in Sydney, Australia. Train stations in City of Sydney are treated as cloud nodes, and suburban train stations act as edge nodes. Each station has a parking with limited available parking lots, which represents the capacity of the node. The length of connected edges are the length of the shortest road between train stations. The dataset contains communication heterogeneity as paths between different nodes can have different charges due to factors such as toll roads and so forth. Parking requests are simulated as tasks which will be allocated to nodes. We pick 20 stations from the City of Sydney to act as cloud nodes, and 30 stations from Sydney suburban areas as edge nodes, numbered from 1 to 20, and from 21 to 50, respectively. We utilize 200 tasks, each with certain amount of parking requests that will be treated as workloads. Parking in the city or in the suburban area can yield different parking fares, which serves as the cost of the task when being executed on the cloud side and edge side, respectively. Finally, successfully allocating each parking task will earn certain profit.

**Parameter setting.** We now introduce parameter settings in two parts: *PECCO* optimization model parameter settings, as well as improved Moth-flame optimizer parameter settings.

*PECCO optimization model parameter setting.* To reflect the communication heterogeneity, we set the communication cost  $w^{CC}$ ,  $w^{CE}$ ,  $w^{EC}$ , and  $w^{EE}$  to have an average of 1, 2, 4, and 6, respectively. Thanks to the powerful network infrastructure equipped in cloud centers, the intra-cloud communication should be the cheapest among communication directions. The download cost should be cheaper than the upload cost and hence the cost is set to reflect this pattern. Finally, due to the limited network capacity between edge devices, it is natural to possess the highest communication cost.

The ratio parameter  $\lambda$  that balances between cost and profit is set to be  $-8$  so that the algorithm can jointly minimize the cost and profit times this negative ratio.

*PECCO-MFI parameter setting.* We set the default allocation upper bound  $ub$  to be 1, and the Moth-flame shape parameter  $b$  to be 1 to comply with  $ub$ . If the shape parameter  $b$  is set to be too small, then the shape of the spiral will be very tight and it will never allocate tasks to some nodes. On the other hand, if  $b$  is too large, then the spiral will be too wide and it may generate offloading strategy which does not make sense. The default number of search candidates, that is, moths, is set to be 30, and the number of iterations is set to be 100 to make the algorithm efficient. The default value of the threshold of the lifetime parameter  $\tau$  is set to be 0.8.

**Experimental setup and hardware configuration.** We compare the *PECCO-MFI* algorithm with two edge-cloud computation offloading algorithms, including the LARAC algorithm, which traverses the shortest path during communication and optimizes the computation cost, as well as GREEDY, which allocates each task to the side that will yield lower objective value, then greedily select the node which has the shortest distance from the initial location of the task. The effectiveness of the *PECCO-MFI* is also compared with 9 swarm-based optimizers, including Bat Algorithm (BAT),<sup>46</sup> Sine Cosine Algorithm (SCA),<sup>47</sup> WOA,<sup>41</sup> cuckoo search algorithm (CS),<sup>48</sup> firefly algorithm (FFA),<sup>40</sup> PSO,<sup>39</sup> grey wolf optimization (GWO),<sup>42</sup> differential evolution (DE)<sup>49</sup> and the original MFO algorithm.<sup>29</sup> To make the experimental results concrete, all experiments are repeated 10 times and the average results are reported.

We implement the method using python 3.8, and conduct all experiments on a server equipped with Intel Core i9 9900K CPU and 32 GB of memory.

## 5.2 | Comparison of objective optimization between algorithm

To verify the effectiveness of the *PECCO-MFI* algorithm in terms of objective optimization, the objective results of the *PECCO-MFI* and 11 compared methods are listed in Table 1. As we can notice, the proposed *PECCO-MFI* algorithm achieves the lowest objective value among all compared

**TABLE 1** Objective value, profit, cost, and the profit-cost ratio of different algorithms

Value	Method					
	LARAC	Greedy	BAT	SCA	WOA	CS
Overall objective	-19253.93	-22615.6	-41317.38	-41496.97	-42489.74	-44088.8
Profit	2650.29	3054.72	5388.28	5407.45	5531.59	5737.87
Cost	1948.38	1822.16	1788.83	<b>1762.64</b>	1762.98	1814.15
Profit/cost ratio	1.36	1.67	3.02	3.07	3.14	3.17
Value	Method					
	FFA	PSO	GWO	DE	MFO	MFI
Overall objective	-44741.63	-45546.13	-46494.95	-46598.59	-45953.91	<b>-48069.48</b>
Profit	5814.99	5915.65	6039.85	6050.26	5969.91	<b>6229.31</b>
Cost	1778.32	1779.07	1823.88	1803.52	1805.37	1765.0
Profit/cost ratio	3.28	3.34	3.32	3.36	3.32	<b>3.53</b>

Note: The MFO stands for the original MFO algorithm, while the MFI stands for the improved *PECCO-MFI* algorithm. The highest value is marked in bold.

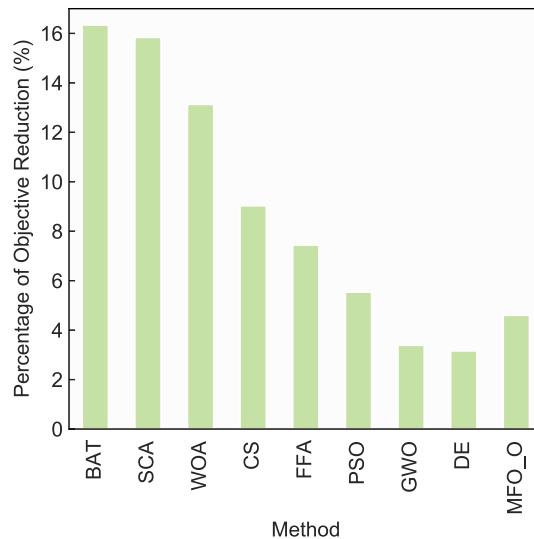


**FIGURE 5** The percentage of objective value reduction achieved by the *PECCO-MFI* algorithm compared with other methods. Since the objective value reduction yielded by the *PECCO-MFI* is 149.7% and 112.6% compared with LARAC and GREEDY, respectively. Therefore, for better visualization, these two methods are omitted from the plot.

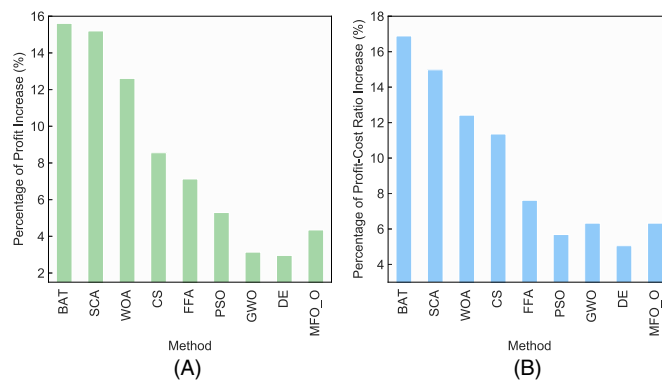


**FIGURE 6** The percentage of increase on profit and profit-cost ratio achieved by the *PECCO-MFI* algorithm compared with other methods are presented in sub-figure (A) and (B), respectively. Since the profit achieved by the *PECCO-MFI* is 135% and 103.9% higher than LARAC and GREEDY, respectively, and the profit-cost ratio is 159.6% and 111.4% higher than LARAC and GREEDY, respectively. Therefore, for better visualization, these two methods are omitted from plots.

methods. As we can observe from Figure 5, the *PECCO-MFI* algorithm produces a 4.6% and 3.16% objective value reduction compared with the original MFO algorithm and the best-performed DE algorithm when tackling this optimization problem, demonstrating the effectiveness of the *PECCO-MFI* algorithm. The significant performance improvement achieved by the *PECCO-MFI* over the original Moth-flame optimizer also verifies the effectiveness of improvements we made on the MFO.

### 5.3 | Comparison of profit and cost between algorithms

After investigating the total objective, we now look at the profit and cost component. As indicated in Table 1 and Figure 6A, the *PECCO-MFI* algorithm achieves the highest profit among all comparing methods. Specifically, the profit achieved is 4.35% and 2.96% higher than the original MFO algorithm, as well as the best-performed DE, respectively. Besides, the *PECCO-MFI* achieves the second lowest cost during computation offloading, which is only 0.1% higher than the SCA algorithm, who has the lowest cost. However, when it comes to the profit-cost ratio, the *PECCO-MFI* yields the best performance. As indicated in Figure 6B, the *PECCO-MFI* algorithm achieves significant profit-cost ratio boost compared with all other methods. The higher the profit-cost ratio is, the more profit will be yielded by spending one unit of cost, that is, the computation offloading is wiser as it

can achieve higher profit by spending unit amount of cost. According to Figure 6B, the *PECCO-MFI* has a profit-cost ratio that is 6.33% and 5.06% superior than the original MFO and DE counterparts, respectively, which demonstrates the effectiveness of the *PECCO-MFI* in terms of profit and cost-oriented offloading optimization. It also indicates that the *PECCO-MFI* can draw a computation offloading strategy that can utilize cost wisely to produce excellent profit.

## 5.4 | Comparison of task allocation between algorithms

We now focus on task allocation done by different algorithms. If offloading in an unwise manner, some computing nodes will be overloaded, causing some tasks failed to be allocated. As we can see from Table 2, the proposed *PECCO-MFI* algorithm achieves the highest task allocation number. A high number of tasks being allocated after computation offloading indicates that the *PECCO-MFI* algorithm can offload tasks wisely without causing severe overloading. Hence, most number of tasks can be successfully allocated and completed instead of being stuck on overloaded computing nodes.

In terms of the profit-allocation ratio, both Table 2 and Figure 7 show that except for the extreme case LARAC due to poor task allocation, the *PECCO-MFI* algorithm produces the highest profit-allocation ratio. The higher the profit-allocation ratio is, the more profit will be yielded by completing each task. As visualized in Figure 7A, the *PECCO-MFI* algorithm achieves 4.26% and 2.03% higher profit-allocation ratio compared with the original MFO and the best-performed DE, respectively. Besides, according to Table 2, the *PECCO-MFI* yields the lowest cost-allocation ratio, which indicates the *PECCO-MFI* causes the lowest cost to satisfy each task, demonstrating its cost-effectiveness. Hence, by achieving the highest number of task allocation, a high profit-allocation ratio and a low cost-allocation ratio, the effectiveness of the offloading strategy yielded by the *PECCO-MFI* algorithm is verified.

**TABLE 2** Number of computation tasks being allocated, the profit-allocation ratio, and the cost-allocation ratio of different algorithms

Value	Method					
	LARAC	Greedy	BAT	SCA	WOA	CS
#Allocation	64.9	92.9	175.3	170.7	177.2	176.7
Profit/allocation ratio	<b>40.96</b>	31.69	30.74	31.68	31.22	32.48
Cost/allocation ratio	30.02	19.61	10.20	10.33	9.95	10.27
Value	Method					
	FFA	PSO	GWO	DE	MFO	MFI
#Allocation	178.6	179.2	179.3	177.6	179.1	<b>179.3</b>
Profit/allocation ratio	32.57	33.69	33.66	34.06	33.33	34.75
Cost/allocation ratio	9.96	9.93	10.17	10.15	10.08	<b>9.84</b>

Note: The highest value is marked in bold.

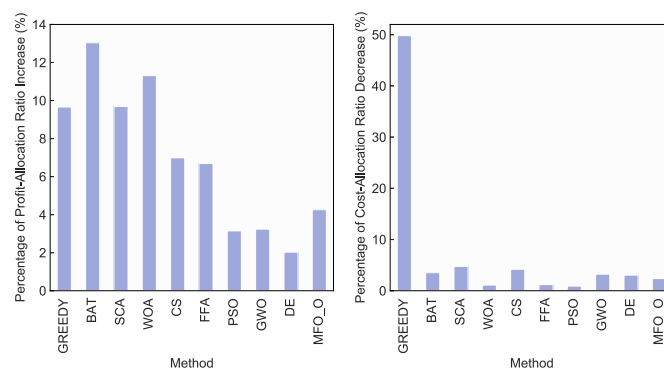


**FIGURE 7** The percentage of profit-allocation ratio increase and cost-allocation ratio decrease achieved by the *PECCO-MFI* algorithm compared with other methods are shown in (A) and (B), respectively. The extreme case LARAC is omitted for better visualization.



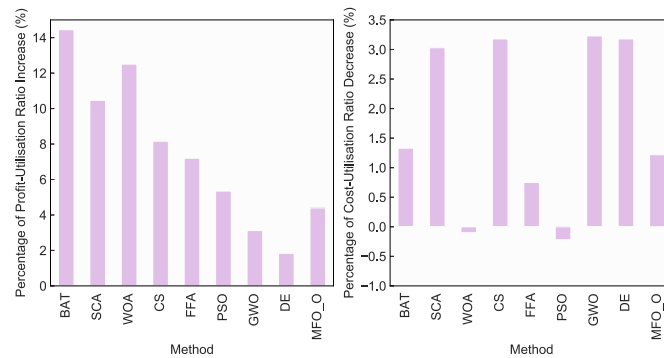
**TABLE 3** Average computing node workload utilization, the profit-utilization ratio, and the cost-utilization ratio of different algorithms

Value	Method					
	LARAC	Greedy	BAT	SCA	WOA	CS
Utilization	121%	112%	95%	92%	95%	95%
Profit/utilization ratio	22.12	32.51	56.97	59.02	57.95	60.28
Cost/utilization ratio	<b>16.10</b>	16.27	18.83	19.16	18.56	19.10

Value	Method					
	FFA	PSO	GWO	DE	MFO	MFI
Utilization	95%	96%	95%	94%	96%	95%
Profit/utilization ratio	60.82	61.89	63.23	64.02	62.45	<b>65.2</b>
Cost/utilization ratio	18.72	18.53	19.20	19.19	18.81	18.58

Note: The highest value is marked in bold.



**FIGURE 8** The percentage of profit-utilization ratio increase and cost-utilization ratio decrease achieved by the *PECCO-MFI* algorithm compared with other methods are shown in (A) and (B), respectively. The extreme cases LARAC and GREEDY are omitted from the plot.

## 5.5 | Comparison of resource utilization between algorithms

Finally, the computing node workload resource utilization, the profit-utilization and cost-utilization ratio are indicated in Table 3. As we can observe, except the LARAC and GREEDY algorithm which overloads some computing nodes, all other methods produce offloading strategy that is free from overloading.

As we can see from Figure 8, the profit-utilization ratio produced by the *PECCO-MFI* algorithm is significantly higher than all other compared methods. Specifically, the *PECCO-MFI* algorithm achieves a 4.4% and 1.8% increase in terms of profit-utilization ratio compared with the original MFO and DE, respectively. The higher the profit-utilization ratio is, the more profit will be yielded by utilizing one unit of computing node resource. On the other hand, the *PECCO-MFI* yields a relatively low cost-utilization ratio, which means the algorithm will not incur a high cost by utilizing one unit of computation resource. Hence, the excellent profit-utilization and cost-utilization ratio indicate the effectiveness of the *PECCO-MFI* algorithm, that is, producing a computation offloading strategy that can utilize computation resource wisely to achieve a high profit and a low cost, without overloading any computing nodes.

## 6 | CONCLUSION

In this article, we propose a profit and cost-oriented edge-cloud computation offloading model *PECCO* which jointly considers the heterogeneous communication and computation cost, as well as the profit yielded after computation offloading. An improved MFO algorithm with three improvements is proposed which addresses several deficiencies of the original MFO and is then integrated to produce an optimized edge-cloud computation offloading strategy, forming the *PECCO-MFI* algorithm. Comprehensive experiments are conducted and the *PECCO-MFI* algorithm is compared with

several other baseline methods to testify to the effectiveness of the PECCO-MFI algorithm when optimizing the edge-cloud computation offloading model, as well as the effectiveness of the improvements made over the original MFO.

## ACKNOWLEDGMENT

This work is supported in part by Key-Area Research and Development Program of Guangdong Province (2020B010164002) and Zhejiang Provincial Natural Science Foundation of China (LZ22F020002).

## DATA AVAILABILITY STATEMENT

The data that support the findings of this study are available from the corresponding author upon reasonable request.

## ORCID

Jiashu Wu  <https://orcid.org/0000-0002-1347-1974>

Yang Wang  <https://orcid.org/0000-0001-9438-6060>

Shigen Shen  <https://orcid.org/0000-0002-7558-5379>

## REFERENCES

- Shafique K, Khawaja BA, Sabir F, Qazi S, Mustaqim M. Internet of things (IoT) for next-generation smart systems: a review of current challenges, future trends and prospects for emerging 5G-IoT scenarios. *IEEE Access*. 2020;8:23022-23040.
- Shen S, Huang L, Zhou H, Yu S, Fan E, Cao Q. Multistage signaling game-based optimal detection strategies for suppressing malware diffusion in fog-cloud-based IoT networks. *IEEE Internet Things J*. 2018;5(2):1043-1054. doi:10.1109/JIOT.2018.2795549
- Zhang K, Tian J, Xiao H, Zhao Y, Zhao W, Chen J. A numerical splitting and adaptive privacy budget allocation based LDP mechanism for privacy preservation in blockchain-powered IoT. *IEEE Internet Things J*. 2022;1. doi:10.1109/JIOT.2022.3145845
- Li T, Wang H, He D, Yu J. Blockchain-based privacy-preserving and rewarding private data sharing for IoT. *IEEE Internet Things J*. 2022;1-1. doi:10.1109/JIOT.2022.3147925
- Wu J, Wang Y, Fan X, Ye K, Xu C. Toward fast theta-join: a prefiltering and amalgamated partitioning approach. *Concurr Comput Pract Exp*. 2021;e6996. doi:10.1002/cpe.6996
- Wu J, Xiong J, Dai H, Wang Y, Xu C. A Multi-Indexing System Based on HDFS for Remote Sensing Data Storage. *Tsinghua Sci Technol*. 2022;27(6):881-893.
- Marjani M, Nasaruddin F, Gani A, et al. Big IoT data analytics: architecture, opportunities, and open research challenges. *IEEE Access*. 2017;5:5247-5261.
- Li M, Wu J, Dai J, et al. A self-contained and self-explanatory DNA storage system. *Sci Rep*. 2021;11(1):1-15.
- Shakarami A, Ghobaei-Arani M, Masdari M, Hosseinzadeh M. A survey on the computation offloading approaches in mobile edge/cloud computing environment: a stochastic-based perspective. *J Grid Comput*. 2020;18(4):639-671.
- Li Q, Zhang Q, Huang H, Zhang W, Chen W, Wang H. Secure, efficient and weighted access control for cloud-assisted industrial IoT. *IEEE Internet Things J*. 2022;1. doi:10.1109/JIOT.2022.3146197
- Shen Y, Shen S, Wu Z, Zhou H, Yu S. Signaling game-based availability assessment for edge computing-assisted IoT systems with malware dissemination. *J Inf Secur Appl*. 2022;66:103140. doi:10.1016/j.jisa.2022.103140
- Ren J, He Y, Huang G, Yu G, Cai Y, Zhang Z. An edge-computing based architecture for mobile augmented reality. *IEEE Netw*. 2019;33(4):162-169.
- Zhang W, Chen J, Zhang Y, Raychaudhuri D. Towards efficient edge cloud augmentation for virtual reality MMOGS. *SEC '17*. Association for Computing Machinery; 2017:1-14.
- Mao Y, You C, Zhang J, Huang K, Letaief KB. Mobile edge computing: survey and research outlook. arXiv preprint arXiv:1701.01090; 2017.
- Yu W, Liang F, He X, et al. A survey on the edge computing for the Internet of Things. *IEEE Access*. 2017;6:6900-6919.
- Shi W, Cao J, Zhang Q, Li Y, Xu L. Edge computing: vision and challenges. *IEEE Internet Things J*. 2016;3(5):637-646.
- Zhao Y, Chen J. A survey on differential privacy for unstructured data content. *ACM Comput Surv*. 2021. doi:10.1145/3490237
- Shi W, Dustdar S. The promise of edge computing. *Computer*. 2016;49(5):78-81.
- Khan WZ, Ahmed E, Hakak S, Yaqoob I, Ahmed A. Edge computing: a survey. *Future Gener Comput Syst*. 2019;97:219-235.
- Dai H, Wu J, Wang Y, Xu C. Towards scalable and efficient Deep-RL in edge computing: A game-based partition approach. *J Parallel Distrib Comput*. 2022;168:108-119. doi:10.1016/j.jpdc.2022.06.006
- Du M, Wang Y, Ye K, Xu C. Algorithmics of cost-driven computation offloading in the edge-cloud environment. *IEEE Trans Comput*. 2020;69(10):1519-1532.
- Wang J, Pan J, Esposito F, Calyam P, Yang Z, Mohapatra P. Edge cloud offloading algorithms: issues, methods, and perspectives. *ACM Comput Surv (CSUR)*. 2019;52(1):1-23.
- Mach P, Becvar Z. Mobile edge computing: a survey on architecture and computation offloading. *IEEE Commun Surv Tutor*. 2017;19(3):1628-1656.
- Wang W, Zhou W. Computational offloading with delay and capacity constraints in mobile edge. Proceedings of the 2017 IEEE International Conference on Communications (ICC); 2017:1-6; IEEE.
- Li Z, Wang C, Xu R. Computation offloading to save energy on handheld devices: a partition scheme. *CASES '01*. Association for Computing Machinery; 2001:238-246.
- Juttner A, Szviatovski B, Mécs I, Rajkó Z. Lagrange relaxation based method for the QoS routing problem. Proceedings IEEE INFOCOM 2001. Conference on Computer Communications. Twentieth Annual Joint Conference of the IEEE Computer and Communications Society (Cat. No. 01CH37213); Vol. 2, 2001:859-868; IEEE.
- Wu H, Knottenbelt W, Wolter K, Sun Y. An optimal offloading partitioning algorithm in mobile cloud computing. Proceedings of the International Conference on Quantitative Evaluation of Systems; 2016:311-328; Springer, New York.
- Dong L, Wang F, Shan J. Computation offloading for mobile-edge computing with maximum flow minimum cut. *CSAE '18*. Association for Computing Machinery; 2018:1-5.

29. Mirjalili S. Moth-flame optimization algorithm: a novel nature-inspired heuristic paradigm. *Knowl Based Syst.* 2015;89:228-249.
30. Liu J, Wang X, Shen S, Yue G, Yu S, Li M. A Bayesian Q-learning game for dependable task offloading against DDoS attacks in sensor edge cloud. *IEEE Internet Things J.* 2021;8(9):7546-7561. doi:10.1109/JIOT.2020.3038554
31. Shi H, Liu S, Wu H, et al. Oscillatory particle swarm optimizer. *Appl Soft Comput.* 2018;73:316-327. doi:10.1016/j.asoc.2018.08.037
32. Lai X, Zhou Y. Analysis of multiobjective evolutionary algorithms on the biobjective traveling salesman problem (1, 2). *Multimed Tools Appl.* 2020;79(41):30839-30860.
33. Davis L. Bit-climbing, representational bias, and test suit design. Proceedings of the International Conference on Genetic Algorithm; 1991:18-23.
34. Lourenço HR, Martin OC, Stützle T. *Iterated local search*. Handbook of Metaheuristics. Springer; 2003:320-353.
35. Ruder S. An overview of gradient descent optimization algorithms. arXiv preprint arXiv:1609.04747, 2016.
36. Goodfellow I, Bengio Y, Courville A. *Deep Learning*. MIT Press. 2016.
37. Li S, Xie B, Wu J, Zhao Y, Liu CH, Ding Z. Simultaneous semantic alignment network for heterogeneous domain adaptation. Proceedings of the 28th ACM International Conference on Multimedia; 2020:3866-3874; Association for Computing Machinery.
38. Keerthi S, Ashwini K, Vijaykumar M. Survey paper on swarm intelligence. *Int J Comput Appl.* 2015;115(5):8-12.
39. Kennedy J, Eberhart R. Particle swarm optimization. Proceedings of ICNN'95-International Conference on Neural Networks; Vol. 4, 1995:1942-1948; IEEE.
40. Yang XS, He X. Firefly algorithm: recent advances and applications. *Int J Swarm Intell.* 2013;1(1):36-50.
41. Mirjalili S, Lewis A. The whale optimization algorithm. *Adv Eng Softw.* 2016;95:51-67.
42. Sm A, Smm B, Al A. Grey Wolf optimizer. *Adv Eng Softw.* 2014;69:46-61.
43. Mirjalili S. Genetic algorithm. *Evolutionary algorithms and neural networks*. Springer; 2019:43-55.
44. Huang D, Fan X, Wang Y, He S, Xu C. DP\_Greedy: a two-phase caching algorithm for mobile cloud services. Proceedings of the 2019 IEEE International Conference on Cluster Computing (CLUSTER); 2019:1-10; IEEE.
45. Transportation N. Commuter Carparks TfNSW open data hub and developer portal; 2021. <https://opendata.transport.nsw.gov.au/dataset/commuter-carparks>. Accessed: January 07, 2021.
46. Yang XS, Gandomi AH. Bat algorithm: a novel approach for global engineering optimization. *Eng Comput.* 2012;29(5):464-483.
47. Mirjalili S. SCA: a sine cosine algorithm for solving optimization problems. *Knowl Based Syst.* 2016;96:120-133.
48. Yang XS, Deb S. Engineering optimisation by cuckoo search. *Int J Math Modell Numer Optim.* 2010;1(4):330-343.
49. Price KV. Differential evolution. *Handbook of Optimization*. Springer; 2013:187-214.

**How to cite this article:** Wu J, Dai H, Wang Y, Shen S, Xu C. PECCO: A profit and cost-oriented computation offloading scheme in edge-cloud environment with improved Moth-flame optimization. *Concurrency Computat Pract Exper.* 2022;e7163. doi: 10.1002/cpe.7163